

Effects of Free-Stream Vorticity on the Blasius Boundary Layer

D.A. Pook, J.H. Watmuff

School of Aerospace, Mechanical & Manufacturing Engineering
 RMIT University, Victoria 3083, Australia

Abstract

CFD results explain the mystery associated with strong streaks in a boundary layer observed experimentally by Watmuff [8] from weak wakes originating upstream of a wind-tunnel contraction. The CFD results show the generation of streamwise vorticity from normal vorticity passing through a wind-tunnel contraction.

Introduction

Watmuff [8] experimentally demonstrated that weak, almost indiscernible non-uniformity in the free-stream can cause significant local thickening of the boundary layer in the region of a wake. Steady wakes ($Re < 40$) were created with thin wires strung perpendicular to the leading edge of the test section flat plate boundary layer.

A wake introduced by a wire in the test section, 7250 diameters upstream, caused a 15% thickening of the boundary layer measured as, $(\delta_{Streak}^* - \delta_{Blasius}^*) / \delta_{Blasius}^*$. Surprisingly, streaks generated from a wire upstream of the wind-tunnel 5:1 two-dimensional contraction caused up to 60% thickening, even though they were an order of magnitude weaker, measured as $\Delta U/U_\infty = 0.1\%$ max. The wakes were also an order of magnitude wider leading Watmuff to suggest the increased sensitivity was possibly due to the boundary layer having a preferred spanwise length scale.

Kogan et. al. [5] conducted a similar experiment to [8] with a wire shedding a vortex street and wakes strengths significantly stronger. A thickening of the boundary layer is observed that becomes spanwise asymmetric with increasing wake strength. Spanwise non-uniformity of the boundary layer has been noted in many experimental studies of transitional and turbulent boundary layers and the effect of screen non-uniformity has been linked indirectly to the spanwise non-uniformity.

Many pre-transitional layers exhibit Klebanoff modes, a low frequency spanwise variation of the layer often visualised as a streak, and often suspected to play a part in bypass transition. Understanding of the results of [8] may provide some insight into streaks in the layer and free-stream disturbances.

Watmuff Experiment Description

Watmuff [8] placed a single wire of diameter, $d = 24.5 \mu m$, $7,250d$ upstream of flat plate with a super-elliptic leading edge. The Re based on wire diameter was 17 thus creating a steady wake that is accurately predicted as a Gaussian profile using the theory of [2], see Figure 1. The wake profile was measured with a total-head tube traverse, 63mm upstream of the leading edge and $\Delta U/U_\infty$ found to be approximately 2%. A steady laminar streak (local thickening of the boundary layer) was observed in the region affected by the wake. A single wire of $d = 254 \mu m$ was then placed $9000d$ upstream of the leading edge, corresponding to 292mm upstream of the wind tunnel 5:1 two-dimensional contraction. The steady wake ($Re_d = 33.9$) from this wire was nearly indiscernible when measure 63mm upstream of the leading edge, $\Delta U/U_\infty = 0.1\%$. However, the width of the wake

was an order of magnitude greater and the corresponding steady streak in the boundary layer was measured to be significantly greater than for the wire in the test section. Assessing the streak in layer as the change in δ^* relative to the undisturbed Blasius value, the test section wire wake streak created approximately a 15% thickening while the upstream of the contraction wire wake produced up to 60% thickening.

Figure 2 visualises the streaks as δ^* surfaces and shows the streak from the upstream wake to grow continually downstream while the test-section wire wake maintains a near constant strength.

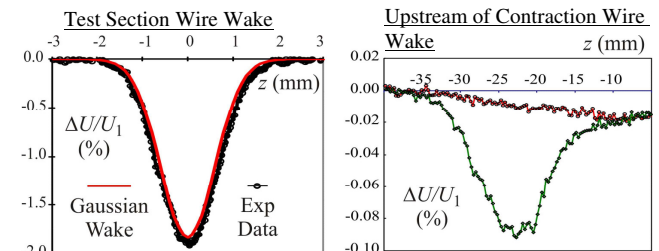


Figure 1. Wakes from wires measured upstream of the leading edge

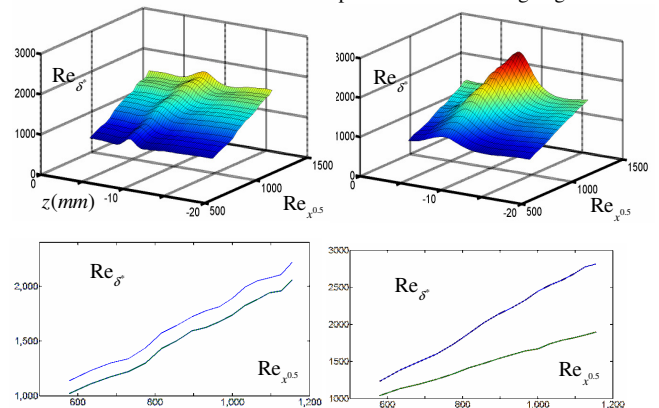


Figure 2. Left-Top: Test section wake streak δ^* surface. Left-Bottom: Streamwise δ^* (Blue in streak, Green undisturbed Blasius). Right-Top: Upstream wake streak δ^* surface. Right-Bottom: Streamwise δ^*

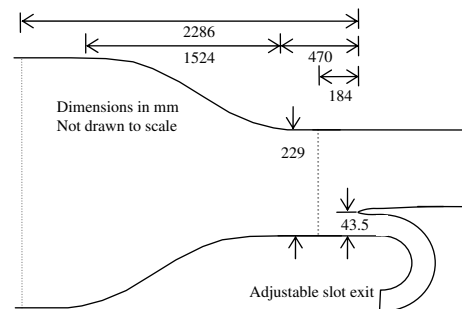


Figure 3: Exp configuration. 5:1, 2D, 5th order polynomial contraction. Super-elliptic leading edge, 3.81 mm half thickness. Dotted lines are wire locations.

CFD Modelling

Fluent 6.3 with 2nd order Pressure, 3rd order MUSCL momentum and SIMPLEC pressure-velocity coupling was used for all cases. A representative mesh size for the leading edge and plate section was 80/140 streamwise nodes respectively and 30 nodes through the laminar Blasius layer and a further 20 within one layer thickness above. 35 nodes within 20mm and 15mm were used in the spanwise direction for the upstream wire streak and test section wire streak respectively. The wake centreline was modelled as symmetry. The side domain was modelled as symmetry, 125mm from the wake centreline. Refinement studies showed no discernable change with mesh density or domain size.

Initial Modelling

Initial CFD modelling simply employed a Gaussian wake velocity profile past a super-elliptic leading edge matching the experiment with two symmetry boundary conditions. It was believed their existed a preferred spanwise length scale of the wake that would produce boundary layer streaks as observed experimentally. Goldstein et al. [4] has analytically analysed the receptivity of flat plate with leading edge to steady normal vorticity and found vortex stretching around the leading edge to be a strong mechanism producing streamwise vorticity downstream distorting the boundary layer.

The CFD inlet wake profile was fitted to the experimental data and was in good agreement with the theory [2]. Initial CFD results assuming the stagnation line to lie on a plane of symmetry did not match the experimental results as shown in Table 1. In particular, no streak was found to occur for the upstream wire wake model.

	Test Section Wire	Upstream of Contraction Wire
Exp	10-15%	50-60%
CFD	1.5%	No Streak

Table 1. Summary of Experiment Vs Initial CFD Results for streak strength

The experimental configuration of [8] is shown in Figure 3. Flow below the leading is directed into the surroundings through a slot to avoid plenum chambers used in associated experiments. The mass flow through the slot below the leading edge could be varied, altering the attachment point, although no data on the attachment point was recorded. The experimental configuration was modelled in CFD, breaking the attachment line symmetry. Increasing slot mass flow moved the attachment point to the topside of the leading edge and substantially increasing the streak strength for the test section wire wake, see Figure 4, with little discernable effect on the flat plate pressure gradient downstream of the leading edge. However, the model wake from the upstream wire still showed little or no effect on the boundary layer.

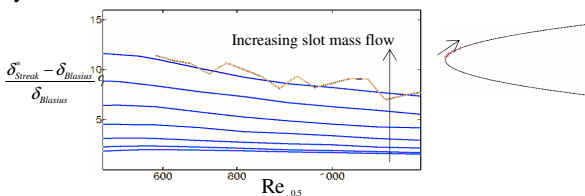


Figure 4. Left: Streak strength versus slot mass flow for test section wake model. Exp. data [8] light brown. Right: Flow attachment positions

Although the location of the attachment point was not recorded experimentally, independent static pressure measurements above the leading edge showed almost no undershoot indicating down-flow onto the leading edge, generated with increased mass flow through the slot. CFD data showed reducing pressure undershoot with increasing slot mass flow ratio.

Contraction Modelling

To reproduce the experimental results for the wire wake upstream of the contraction, a separate contraction mesh was used to produce a new inlet boundary condition to the leading edge mesh. The contraction mesh had 5mm node spacing in the streamwise direction, 110 in the wall-normal and 80 in the spanwise directions. The centre symmetry plane of the wake was utilized and the far-side symmetry boundary condition was 200mm from the wake centreline and not found to affect results.

The contraction introduces new parameters not measured in [8], including the boundary layer thickness entering and exiting the contraction. Two-dimensional modelling showed the thickness of the boundary layer exiting the contraction was essentially independent of the thickness entering. Flow past a cylinder junction with a wall will generate streamwise vorticity in the downstream boundary layer. The important flow parameters are Re_d and δ^*/d , studied over the range $Re_d = 33.9$, $1.0 < \delta^* < 2.24$ mm ($3.9 < \delta^*/d < 8.8$). CFD results did not indicate the presence of a laminar horse-shoe vortex, in accordance with Baker [4], although weak streamwise vorticity was still present in the downstream boundary layer. The wake flow through the contraction for varied δ^*/d exited the contraction with minimal variation in $\Delta U/U_\infty$ at the height of the leading edge in accordance with [8] and minimal variation in the streamwise vorticity approaching the leading edge (see Figure 5) eliminating the need to consider the boundary layer thickness at the wire wall junction. Streamwise vorticity was present in the flow exiting the contraction with a region of maximum counter-rotating streamwise vorticity located above the tunnel floor boundary layer as shown in Figure 6, left. Opposite rotating streamwise vorticity maximums, approximately 5 times weaker, are seen in the contraction floor boundary layer. The streamwise vorticity above the layer appears to evolve from the contraction boundary layer in the concave curvature region, as visualised by in-plane contours in Figure 7.

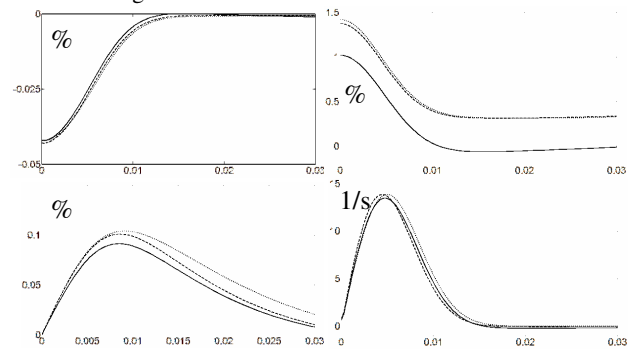


Figure 5. CFD, Spanwise profiles 63mm upstream of leading edge. Horizontal scale is spanwise position (m) with symmetry of wake at 0. Solid- $\delta^*/d=3.8$, Dash- $\delta^*/d=5.0$, Dot- $\delta^*/d=8.8$. Top Left: $\Delta U/U_\infty$. Top Right: v/U_∞ . Bottom Left: w/U_∞ . Bottom Right: Streamwise Vorticity

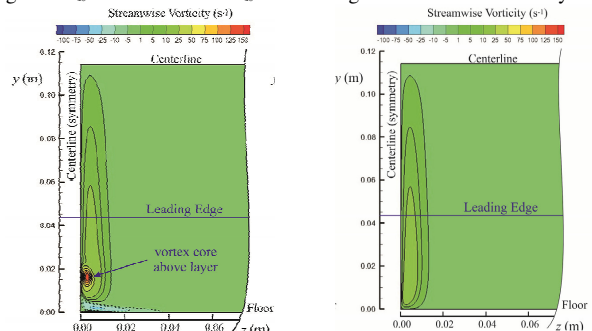


Figure 6. Contours of streamwise vorticity 407mm from contraction exit (63mm before leading edge). Left- Contraction with floor boundary layer. Right- Contraction with Slip floor (no boundary layer)

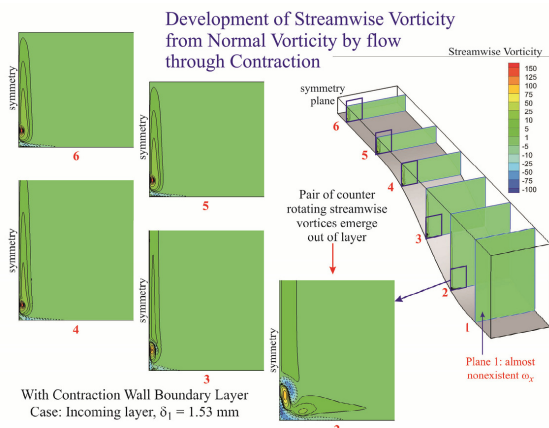


Figure 7. Contours of streamwise vorticity on planes through contraction with floor boundary layer

Contraction Wake With Leading Edge

A plane 70mm downstream of the contraction exit (400mm before the plate leading edge) in a region of low streamwise pressure gradient was taken as the inlet boundary condition to the leading edge CFD mesh. The boundary layer response to wire wake passed through the contraction, producing a wake with minimal $\Delta U/U_\infty$ variation, was found to produce significant thickening of the test section boundary layer in accordance with experiment [8]. The peak regions of streamwise vorticity pass below the plate leading edge.

Figure 5 shows the velocity profiles 63mm upstream of the leading edge. Perturbation of the normal velocity component is seen to be significantly larger than the streamwise component but still only approximately 1% of the free-stream velocity making detection in the experiment difficult.

The slot mass flow was adjusted to match both the wire in the test section and wire upstream of the contraction cases. The test section wire case was recalculated to include the wire and leading edge in a single mesh, allowing for upstream influence of the leading edge on the wire and to ensure the mass flow effects of the wind tunnel floor boundary layer were taken into account properly. Increasing slot mass flow alters the flow upstream of the leading edge, bending streamlines down and thus producing a slightly non-uniform wake with respect to position along the test section wire. Increasing the slot mass flow was found to reduce the boundary layer streak for the wake produced by the wire upstream of the contraction while the opposite effect was observed for the test section wire wake. Figure 8 shows the experimentally measured streak development for both the upstream and test-section wire cases and the CFD matching with the same slot mass flow for both cases, found via trial and error and causing a slight down-flow at the leading edge. Of note, the test section wire wake normal vorticity is a factor of 10 greater than the streamwise component of upstream of the contraction wire wake, measured 63mm before the leading edge.

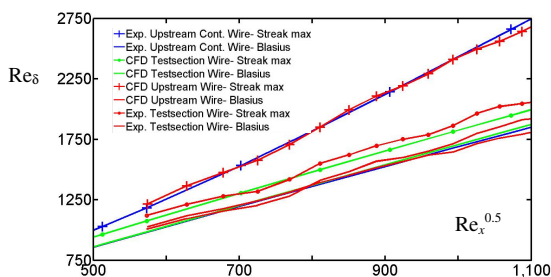


Figure 8. Agreement between CFD and Exp results

Streak Generation via Normal & Streamwise Vorticity

The thickening of the boundary layer streak for the two cases of a wire in the test section and wire upstream of the contraction represent streak generation via normal vorticity and streamwise vorticity respectively. The normal vorticity streak shows rapid growth in the region of the leading edge before decaying downstream, see Figure 4. Increasing the slot mass flow and effectively tilting the normal oriented vorticity prior to the plate and producing a streamwise component produces a stronger streak downstream. The streamwise vorticity streak shows continual growth over the length of the flat plate as shown in Figure 9. Increasing the slot mass flow ratio tilts the vorticity and creates a normal component which reduces the streak strength seen downstream in the boundary layer.

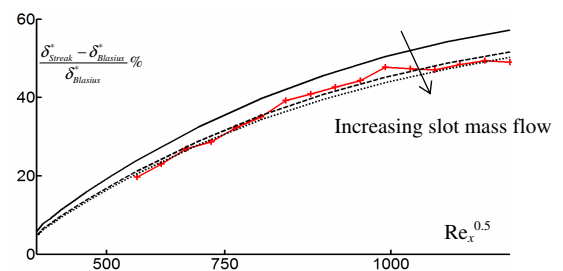


Figure 9. Streak growth for upstream wire wake. Exp data shown in red

Clearly continual forcing of the boundary layer from weak steady streamwise vorticity will lead to larger amplitude streaks and a greater spanwise non-uniformity. Recently published DNS results by Schrader et al. [6] similarly find that the boundary layer is most receptive to low frequency, particularly steady, streamwise vorticity.

Wind-tunnel contractions provide a mechanism for normal orientated vorticity to become streamwise oriented. The results presented here and by [6] highlight the strong influence of streamwise vorticity on the boundary layer. A prime source of normal vorticity upstream of a wind tunnel contraction is the settling chamber screens. Utilizing a contraction to reduce the incoming flow non-uniformity in an effort to improve the flow quality could lead to a greater spanwise non-uniformity in the test section boundary layer.

Streamwise Vorticity Creation in the Contraction

Lanspeary & Bull [3] experimentally observed the creation of a streamwise vortex pair above the boundary layer in a three-dimensional contraction due to flow separation. They conclude flow non-uniformities entering the contraction are amplified by a Görtler instability, forming streaks that merge downstream due to lateral pressure gradients in their complex 3d contraction, with a counter-rotating vortex pair eventually leaving the boundary layer. Placing a series of screens in the contraction past the concave region into the positive pressure gradient region prevented the occurrence of the streamwise vorticity above the boundary layer.

The current CFD results do not show any separation yet steady counter rotating streamwise vorticity is observed exiting the contraction. Figure 10 shows the maximum streamwise vorticity in a given streamwise plane through the contraction. Minimal streamwise vorticity is present at the start of the contraction from the wire/wake flow junction. Through the concave region of the contraction large growth in streamwise vorticity is observed before decaying as the curvature of the contraction is reduced. The maximum is located near the contraction floor and presumably generated via the turning of the flow near the floor.

The opposite rotating streamwise vorticity in the layer also increase rapidly before a stronger decay due to its presence in the boundary layer. The second region of streamwise vorticity growth is presumably due to vortex stretching in the positive pressure gradient region while the final decay, beginning just prior to the contraction exit is due to the flow turning back. The opposite rotating streamwise vorticity in the layer grows to a significantly smaller amplitude due to its lower starting value and soon decays after the contraction.

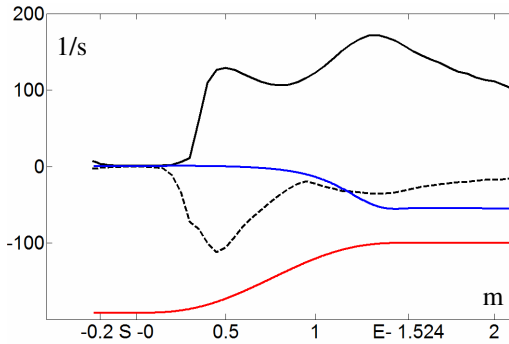


Figure 10. Solid Black- peak streamwise vorticity above the contraction boundary layer. Dashed black- peak streamwise vorticity in the layer, Blue- static pressure. Red- outline of contraction shape. S, E- Start/end of contraction curvature.

The screens placed into the contraction by [4] possibly minimised the streamwise vorticity incoming, hence there was minimal streamwise vorticity present to stretch in the mid section of the contraction

Streamwise Vorticity Creation- Slip Floor Contraction

A series of CFD solutions utilising the same contraction geometry with a slip-wall and two-dimensional incoming wake predicted by theory from the upstream wire was conducted for three contraction ratios. This prevents the creation of a boundary layer in the contraction. The 5:1 contraction ratio simulation with a slip-wall shows significant streamwise vorticity exiting but without the strong cores present when a boundary layer is present in the contraction, see Figure 6. The streamwise and normal vorticity in the vicinity of the leading edge is found to be near identical and the test section plate boundary layer was found to have the same downstream thickening. Figure 11 shows the streamwise vorticity created in the contraction with a slip floor and the normal vorticity decay for various contraction ratios.

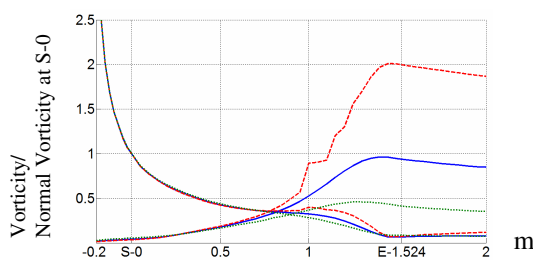


Figure 11. Peak streamwise vorticity growth and normal vorticity decay in a slip-wall contraction. Blue solid- 5:1 contraction ratio. Green dot- 2.5:1, Red Dash- 10:1

A small amount of streamwise vorticity is generated prior to the curvature of the contraction. Prior to the contraction a small x-velocity gradient in the wall normal direction is present, tilting the incoming normal vorticity and creating streamwise vorticity via the following term of the vorticity transport equations.

$$\omega_y \frac{\partial u}{\partial y} \quad (1)$$

At the exit of the contraction the x-velocity gradient changes sign and a reduction in streamwise vorticity can be observed. The 5:1

contraction exhibits a peak streamwise vorticity exiting that is 93% of the peak normal vorticity entering. Doubling/halving the contraction ratio approximately doubles/halves this ratio, presumably due to differing vortex stretching in the favourable pressure gradient region. The peak normal vorticity exiting shows little variation with contraction ratio suggesting a smaller contraction ratio would produce flow of near same $\Delta U/U_\infty$ uniformity with less streamwise vorticity to cause spanwise perturbations of the test section boundary layer. The results also indicate that an incoming boundary layer to the contraction with streamwise vorticity present is not required to produce significant streamwise vorticity downstream of the contraction.

Conclusion

CFD results explain the mystery associated with the strong effect of the weak wakes originating upstream of the contraction in the experimental results of Watmuff [4]. For these cases the CFD clearly shows how the normal vorticity is transformed into streamwise vorticity when the wakes pass through the contraction. Recent results by Schrader et. al. [6] confirm the greater receptivity of boundary layers to streamwise vorticity compared to normal vorticity. Tilting of the vorticity by introducing an effective angle of attack can substantially alter the boundary layer response. Utilising a wind tunnel contraction to reduce the flow non-uniformity in the test section as measured by $\Delta U/U_\infty$ may increase the spanwise non-uniformity of the test section boundary layer due to the creation of streamwise vorticity. It has long been noted by experimentalists that wind tunnel settling screens, in particular their 'quality' and uniformity, is linked to undesired disturbances in the test section such as spanwise variation and Klebanoff modes. Further work is being conducted to extend the current CFD analysis to wakes more representative of wind tunnel settling screens in order to better predict boundary layer disturbances caused by non-uniformity in the free stream.

References

- [1] Baker, C.J., The Laminar Horseshoe Vortex, *J. Fluid Mech.*, **95**, 1979, 347-367
- [2] Batchelor, G.K., *An Introduction to Fluid Mechanics*, Cambridge University Press, 1967
- [3] Lanspeary, P.V. & Bull, M.V., A Mechanism for Laminar Three-Dimensional Separation in Duct Contractions, 13th Australasian Fluid Mechanics Conference, 13-18 Dec 1998
- [4] Goldstein, M.E., Leib, S.J., & Cowley, S.J., Distortion of a Flat-Plate Boundary Layer by Free-Stream Vorticity Normal to the Plate, *J. Fluid Mech.*, **237**, 1992, 231-260
- [5] Kogan, .N., Shumilkin, V.G., Ustinov, M.V. & Zhigulev, S.V., Response of Boundary Layer Flow to Vortices Normal to the Leading Edge', *Euro. J. Mech.-B/Fluids*, **20**, 2001, 813-820
- [6] Schrader, L.U., Brandt, L., Marvriplis, C. & Henningson, D.S., Receptivity of free-stream vorticity of flow past a flat plate with elliptic leading edge, *J. Fluid Mech.*, **653**, 2010, 245-271
- [7] Watmuff, J.H. Detrimental Effects of Almost Immeasurably Small Freestream Nonuniformities Generated by Wind-Tunnel Screens, *AIAA J.*, **36**, 1998, 379-386
- [8] Watmuff, J.H., Effects of Weak Freestream Nonuniformity on Boundary Layer Transition, *J. Fluid. Eng.*, **128**, 2006, 247-257

